

Condensation and criticality of eigen microstates of phase fluctuations in Kuramoto model

Ning-Ning Wang(王宁宁), Qing Yao(姚卿), Ying Fan(樊瑛), Zeng-Ru Di(狄增如), and Xiao-Song Chen(陈晓松)
Citation: Chin. Phys. B, 2025, 34 (**10**): 100501. DOI: 10.1088/1674-1056/addd84
http://cpb.iphy.ac.cn; http://iopscience.iop.org/cpb

What follows is a list of articles you may be interested in

Effects of noise on synchronization in simplicial complexes

Linying Xiang(项林英), Shuwei Yao(姚姝玮), Yining Chen(陈艺宁), Ruitong Yan(闫锐桐), and Ruya Xia(夏儒雅)
Chin. Phys. B, 2025, 34 (**7**): 070503. DOI: 10.1088/1674-1056/adc7ef

Optimal synchronization of higher-order Kuramoto model on hypergraphs

Chong-Yang Wang(王重阳), Bi-Yun Ji(季碧芸), and Linyuan Lü(吕琳媛)
Chin. Phys. B, 2025, 34 (**7**): 070502. DOI: 10.1088/1674-1056/adcded

Synchronous dynamics of robotic arms driven by Chua circuits

Guoping Sun(孙国平), Mingxin Xu(许明鑫), Guoqiang Jin(金国强), and Xufeng Wang(王旭峰)
Chin. Phys. B, 2025, 34 (**6**): 060501. DOI: 10.1088/1674-1056/adc2e1

Effects of potential field delay and coupling delay on collective behavior of a fractional-order coupled system in a dichotomous fluctuating potential

Yangfan Zhong(钟扬帆), Xi Chen(陈熙), Maokang Luo(罗懋康), and Tao Yu(蔚涛)
Chin. Phys. B, 2025, 34 (**5**): 050501. DOI: 10.1088/1674-1056/adbd15

Effects of asymmetric coupling and boundary on the dynamic behaviors of a random nearest neighbor coupled system

Ling Xu(徐玲) and Lei Jiang(姜磊)
Chin. Phys. B, 2024, 33 (**6**): 060503. DOI: 10.1088/1674-1056/ad3b86

Condensation and criticality of eigen microstates of phase fluctuations in Kuramoto model

Ning-Ning Wang(王宁宁)[1,2], Qing Yao(姚卿)[3], Ying Fan(樊瑛)[3], Zeng-Ru Di(狄增如)[3,4], and Xiao-Song Chen(陈晓松)[3,5,†]

[1] *School of Artificial Intelligence, Tiangong University, Tianjin* 300387, *China*
[2] *School of Mathematical Science, Nankai University, Tianjin* 300071, *China*
[3] *School of Systems Science, Beijing Normal University, Beijing* 100875, *China*
[4] *International Academic Center of Complex Systems, Beijing Normal University, Zhuhai* 519087, *China*
[5] *Institute for Advanced Study in Physics and School of Physics, Zhejiang University, Hangzhou* 310058, *China*

(Received 27 April 2025; revised manuscript received 25 May 2025; accepted manuscript online 28 May 2025)

The Kuramoto model is one of the most profound and classical models of coupled phase oscillators. Because of the global couplings between oscillators, its precise critical exponents can be obtained using the mean-field approximation (MFA), where the time average of the modulus of the mean-field is defined as the order parameter. Here, we further study the phase fluctuations of oscillators from the mean-field using the eigen microstate theory (EMT), which was recently developed. The synchronization of phase fluctuations is identified by the condensation and criticality of eigen microstates with finite eigenvalues, which follow the finite-size scaling with the same critical exponents as those of the MFA in the critical regime. Then, we obtain the complete critical behaviors of phase oscillators in the Kuramoto model. We anticipate that the critical behaviors of general phase oscillators can be investigated by using the EMT and different critical exponents from those of the MFA will be obtained.

Keywords: synchronization, coupled oscillators, eigen microstate, criticality

PACS: 05.45.Xt, 05.70.Fh, 64.60.Ht

DOI: 10.1088/1674-1056/addd84 **CSTR:** 32038.14.CPB.addd84

1. Introduction

Synchronization phenomena exist in various types of systems, from biological systems such as the flashing fireflies to social systems, such as business cycles in economics,[1] to neuronal systems, such as the periodic firing of neurons in the brain.[2] The transition from disorder to synchronization or partial synchronization usually characterizes a change in a system's function or properties,[3–5] i.e., the patterns of partial synchronization in brain networks are linked to different brain functions. Therefore, it is essential to understand the mechanism behind the emergence of synchronization.

The Kuramoto model is one of the most fundamental and classical models of coupled oscillators for studying synchronization phenomena. For the Kuramoto model, in the mean-field approximation (MFA), the Ott-Antonsen ansatz[6] and self-consistent equation method are the classic theoretical research routes followed.[7,8] Using those methods, the model and its extended versions have been widely studied to explore their critical behaviors analytically.[9–11] The MFA can provide precise critical exponents for high-dimensional systems or long-range coupled systems so that Ginzburg's criterion is satisfied.[12] In general, precise critical behaviors cannot be obtained under the MFA. This poses a big challenge to the studies of phase transition in heterogeneous and nonequilibrium systems, since their emergent phases can be heterogeneous and evolve over time. Particularly in the study of finite-size scaling (FSS), the time average of the order parameter often only utilizes the modulus, neglecting the phase angle, which leads to inaccurate measurement of the system orderliness. To address the shortcomings of the above analysis method, this paper investigates the criticality of the Kuramoto model on FSS using the eigen microstate. In the eigen microstate theory (EMT) developed by Chen *et al.*,[13–20] the emergence of phase is equivalent to the condensation of an eigen microstate in a statistical ensemble, indicated by the finite eigenvalue, which is also the order parameter of phase transition. Compared with the statistical mechanics of Gibbs, the EMT account for the distribution function of eigen microstates rather than microstates.

In previous studies, the EMT has been applied to the Ising and percolation models[13–15] and has obtained the same critical exponents. Regarding the phase transition type of the Vicsek model for collective motion, it was disputed whether the phase transition is continuous or discontinuous. Using the EMT, it has been demonstrated that there are actually two phase transitions in the Vicsek model. As noise decreases, there is a discontinuous phase transition of density at first and then a continuous phase transition of collective

†Corresponding author. E-mail: chenxs@bnu.edu.cn

© 2025 Chinese Physical Society and IOP Publishing Ltd. All rights, including for text and data mining, AI training, and similar technologies, are reserved.

motion.[17] In addition, the EMT has also been applied to climate systems, such as Earth's system temperature, ozone distribution and atmospheric structure, chimera states and epidemic models,[16,21–24] and even revealing the structure and functional mechanisms of the human brain.[25,26] The spatial distributions of eigen microstates can describe the structures of macroscopic, mesoscopic, and microscopic scales and the corresponding time evolutions. These are very helpful for understanding the mechanisms behind their emergence in complex systems.

As an important supplement to the order parameter dynamics in complex systems,[27] we apply the EMT to revisit the phase transition from disorder to synchronization in the Kuramoto model. Using the phase translational invariance, the microstate configuration in the EMT is established. Through experiments, we obtain the same critical properties as the MFA, such as the critical coupling strength and critical exponents. Moreover, the eigen microstates and their evolutions can visually represent the oscillators' spatial distribution, phase separation, and their principal fluctuation modes. It has been demonstrated that the emergence of the largest eigen microstate indicates synchronization, which also evolves with time and is consistent with the fact that the Kuramoto model is not in equilibrium.

This paper is organized as follows. Section 2 introduces the Kuramoto model and defines its microstates. Then, we provide the finite-size scaling of eigenvalues and calculate the critical exponents of the Kuramoto model in Section 3. Section 4 demonstrates the spatial and temporal patterns of eigen microstates for different coupling strengths. Finally, we present our conclusions and discussions in Section 5.

2. Kuramoto model and its microstates

The Kuramoto model consisting of a finite population of N globally coupled oscillators is governed by

$$\dot{\theta}_i = \omega_i + \frac{K}{N}\sum_{j=1}^{N}\sin(\theta_j - \theta_i), \quad i = 1,2,\ldots,N, \tag{1}$$

where θ_i and ω_i are the phase and intrinsic frequency of oscillator i, and K is the coupling strength. The equation demonstrates the two competing tendencies of an oscillator, one is to rotate according to its intrinsic frequency, and the other is to shrink the differences between its own phase and its neighbors' (in the globally coupled case, its neighbors include all other oscillators). When the coupling strength is weak, the oscillators keep their periodic motion. With an increase of coupling strength, more and more oscillators will be synchronized.

To quantify the coherence of oscillators, Kuramoto introduced the following order parameter and defined it as

$$z = \Delta\, \mathrm{e}^{\mathrm{i}\Theta} = \frac{1}{N}\sum_{j=1}^{N}\mathrm{e}^{\mathrm{i}\theta_j}, \tag{2}$$

where Δ is the modulus of this complex order parameter and Θ is the arbitrary phase of oscillator. If the oscillator's phases are uniformly distributed in the range $[-\pi,\pi]$, $\Delta = 0$, meaning no synchrony among the oscillators. If all oscillators rotate with the same phase, there is the full synchrony and $\Delta = 1$. In most cases of phase distribution, $0 < \Delta < 1$ and oscillators are partially synchronized.

Inserting Eq. (2) into Eq. (1), we obtain

$$\dot{\theta}_i = \omega_i + K\Delta\sin(\Theta - \theta_i), \quad i = 1,2,\ldots,N. \tag{3}$$

If the coupling strength K is extremely weak, $\Delta \approx 0$ and this equation can be regarded as a dynamic equation of a simple driven pendulum without damping. With the increase of K, there exists a critical value K_c so that some oscillators start to rotate at the same pace $\Theta = \bar{\omega}t$ for $K \geq K_\mathrm{c}$ (the mean frequency $\bar{\omega}$ is not directly equal to the average of intrinsic frequencies $\langle\omega_i\rangle$. It is merely the angular velocity of the synchronous motion of the coherent oscillator, affected by the intrinsic frequency and the coupling structure dynamics). The phase order parameter is strictly zero on the subcritical side $(K < K_\mathrm{c})$. Based on the self-consistent equation, the critical coupling strength and its scaling exponent β can be rigorously calculated through theoretical derivation.[7] On the supercritical side $(K > K_\mathrm{c})$, the order parameter obeys $\Delta \propto (K - K_\mathrm{c})^{\beta}$ with $\beta = 0.5$. Generally, for an even and unimodal intrinsic frequency distribution, the critical coupling strength of the Kuramoto model is

$$K_\mathrm{c} = \frac{2}{\pi g(0)}. \tag{4}$$

From the definition of order parameter in the mean-field, we can observe that the order parameter z is a time-evolving complex-valued signal. However, in finite-scale studies, scholars often characterize the orderliness of system through the time average $\langle\Delta\rangle$ of modulus $\Delta(t)$, which loses the phase information. Near the critical state, we obtain the amplitude Δ and phase barycenter $\bar{\theta}$ of the order parameter z in Figs. 1(a) and 1(c), as well as their Fourier amplitude spectrum and phase spectrum in Figs. 1(b) and 1(d), through numerical simulations after the system has stabilized. The state evolution shown by the amplitude and phase barycenter both correspond to the condensation of the Fourier frequency spectrum. By integrating the amplitude and phase information, we introduce the EMT to characterize the system's orderliness.

In the EMT,[13,15,16] the ensemble is composed of microstates, which describe the states of all components in a

system. For the Kuramoto model, we define the state of an oscillator by its phase deviation from the barycenter $\bar{\theta}^I$,

$$\bar{\theta}^I = \arctan 2\left(\frac{1}{N}\sum_i \sin\theta_i^I, \frac{1}{N}\sum_i \cos\theta_i^I\right), \tag{5}$$

where $\arctan 2(y,x)$ is inverse tangent function in four quadrants, which is consistent with the calculation method of the phase barycenter in higher-order models.[28] The phase translation of oscillators around this center is more convenient for measuring the phase dynamic coherence. Particularly in the study of multiple synchronized clusters, the offset of the oscillator centroid is often unsuitable for directly depicting the phase transition, requiring the introduction of higher-order order parameters.[29,30] Inspired by studies of chimera states[24] and the XY model,[31] we define the state of oscillator i at time I as

$$S_i^I = \left({}_cS_{i,s}^I S_i^I\right)^{\mathrm{T}} = \left(\cos(\delta\theta_i^I), \sin(\delta\theta_i^I)\right)^{\mathrm{T}}, \tag{6}$$

where $\delta\theta_i^I = \theta_i^I - \bar{\theta}^I$.

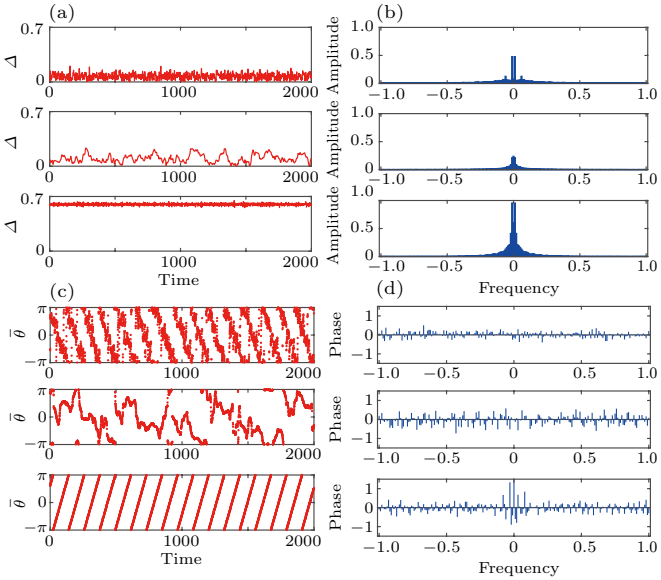


Fig. 1. The evolution of (a) amplitude Δ and (c) phase barycenter $\bar{\theta}^I$ over time near the critical state and (b), (d) their Fourier spectra results. Results are shown for three coupling strengths: critical ($K_c = \sqrt{8/\pi} = 1.5958$) and near-critical $(1\pm0.1)K_c$).

Using M microstates, we can construct a statistical ensemble described by a $2N\times M$ normalized matrix $\boldsymbol{A}$ with elements

$$A_i^I = \frac{S_i^I}{\sqrt{C_0}}, \tag{7}$$

where $C_0 = N\times M$. Thus, we can obtain an $M\times M$ correlation matrix of microstates

$$\mathcal{C} = C_0\boldsymbol{A}^{\mathrm{T}}\cdot\boldsymbol{A}, \tag{8}$$

where the matrix element C_{IJ} represents the correlation between the microstates I and J defined as

$$C_{IJ} = (\boldsymbol{S}^I)^{\mathrm{T}}\boldsymbol{S}^J = \sum_i \cos\left(\delta\theta_i^I - \delta\theta_i^J\right), \tag{9}$$

$\boldsymbol{S}^I = \left(S_i^I, S_2^I, \ldots, S_N^I\right)^{\mathrm{T}}$, and its trace $\mathrm{Tr}\,\boldsymbol{C} = C_0$. Similarly, the correlations between different oscillators are described by a $2N\times 2N$ matrix

$$\boldsymbol{K} = C_0\boldsymbol{A}\cdot\boldsymbol{A}^{\mathrm{T}}, \tag{10}$$

with the correlation between the oscillators i and j

$$\begin{aligned} K_{ij} &= \boldsymbol{S}_i(\boldsymbol{S}_j)^{\mathrm{T}} \\ &= \begin{pmatrix} \sum_I \cos(\delta\theta_i^I)\cos(\delta\theta_j^I) & \sum_I \cos(\delta\theta_i^I)\sin(\delta\theta_j^I) \\ \sum_I \sin(\delta\theta_i^I)\cos(\delta\theta_j^I) & \sum_I \sin(\delta\theta_i^I)\sin(\delta\theta_j^I) \end{pmatrix}, \end{aligned} \tag{11}$$

where $\boldsymbol{S}_i = \left(S_i^1, S_i^2, \ldots, S_i^M\right)$ and its trace $\mathrm{Tr}\boldsymbol{K} = C_0$.

The correlation matrix $\boldsymbol{C}$ has M eigenvectors $\boldsymbol{V}_I$ of $I = 1,2,\ldots,M$, which form an $M\times M$ unitary matrix $\boldsymbol{V} = [\boldsymbol{V}_1, \boldsymbol{V}_2, \ldots, \boldsymbol{V}_M]$. The correlation matrix $\boldsymbol{K}$ has $2N$ eigenvectors $\boldsymbol{U}_i$ of $i = 1,2,\ldots,2N$, which form a $2N\times 2N$ unitary matrix $\boldsymbol{U} = [\boldsymbol{U}_1, \boldsymbol{U}_2, \ldots, \boldsymbol{U}_{2N}]$. Through the singular value decomposition, the ensemble matrix $\boldsymbol{A}$ can be factorized as

$$\boldsymbol{A} = \boldsymbol{U}\cdot\boldsymbol{\Sigma}\cdot\boldsymbol{V}^{\mathrm{T}}, \tag{12}$$

where $\boldsymbol{\Sigma}$ is a $2N\times M$ diagonal matrix with elements

$$\Sigma_{IJ} = \begin{cases} \sigma_I, & \text{for } I = J \leqslant r, \\ 0, & \text{for otherwise}, \end{cases} \tag{13}$$

with the I-th eigenvalue σ_I and $r = \min(M, 2N)$. As a result, the ensemble matrix $\boldsymbol{A}$ can be rewritten in terms of the eigenvectors $\boldsymbol{U}$ and $\boldsymbol{V}$ using their tensor product

$$\boldsymbol{A} = \sum_{I=1}^{r}\sigma_I\boldsymbol{A}_I^{\mathrm{e}} = \sum_{I=1}^{r}\sigma_I\boldsymbol{U}_I\otimes\boldsymbol{V}_I. \tag{14}$$

From the statistical ensemble $\boldsymbol{A}$, we can obtain not only the eigen microstates $\boldsymbol{U}_I$, quantifying the collective behaviors of system, but also the eigen dynamic microstates $\boldsymbol{V}_I$, describing the temporal evolution of $\boldsymbol{U}_I$. Since $\mathrm{Tr}\boldsymbol{C} = \mathrm{Tr}\boldsymbol{K} = C_0$, we have

$$\sum_{I=1}^{r}\sigma_I^2 = 1, \tag{15}$$

and $w_I = \sigma_I^2$ defines the probability of the eigen ensemble $\boldsymbol{A}_I^{\mathrm{e}}$ in the statistical ensemble $\boldsymbol{A}$. Naturally, we can consider σ_I as the order-parameter of the eigen microstate $\boldsymbol{U}_I$.

3. Finite-size scaling of eigenvalues in the Kuramoto model

3.1. The finite-size scaling of eigenvalues

Near the critical point, the FSS of eigenvalues has been proposed and confirmed using Ising models.[13,15,16] Here, the

eigenvalues of the Kuramoto model near the critical point should have the FSS form

$$\sigma_I(K,N) = N^{-\beta/\bar{\nu}} f_I(\varepsilon N^{1/\bar{\nu}}), \tag{16}$$

where β is the critical exponent of the order-parameter, $\bar{\nu} = d\nu$, d is the system dimension, ν is the critical exponent of correlation length, and $\varepsilon = (K - K_c)/K_c$. The function f_I is the finite scaling function for the I^{th} eigenvalue. In the limit $N \to \infty$, the first eigenvalue has the bulk limit

$$\sigma_1(K,\infty) = \begin{cases} a\,\varepsilon^{\beta}, & \varepsilon \geq 0, \\ 0, & \varepsilon < 0. \end{cases} \tag{17}$$

In studies of the Ising model in Refs. [13,15], the ratio $\sigma_I/\sigma_J \equiv R_{I/J}$ of eigenvalues σ_I and σ_J has been investigated and has the FSS form

$$\sigma_I/\sigma_J = R_{I/J}(\varepsilon N^{1/\bar{\nu}}). \tag{18}$$

At the phase transition point, the ratio $R_{I/J}(0)$ is independent of system scale N and is supposed to be universal. The fixed point of $R_{I/J}$ can be used to determine the phase transition point. The exponent $\bar{\nu}$ can be estimated by the scaling form in Eq. (18). Further, the exponent β can determined by Eq. (16).

3.2. Results of the Kuramoto model

In the phase oscillator Kuramoto model, the intrinsic frequency distribution $g(\omega)$ plays a crucial role in the phase transition. Its second derivative $g''(\omega)$ determines the continuity of system phase transition. In this paper, without loss of generality, we arbitrary choose a standard normal distribution $g(\omega) = (1/\sqrt{2\pi})\,\mathrm{e}^{-\omega^2/2}$ and then obtain the critical coupling strength $K_c = 2/\pi g(0) = \sqrt{8/\pi}$ based on Eq. (4). We generate the intrinsic frequency ω_i of oscillator i randomly in each sample and integrate the Kuramoto model numerically for over 500 samples. The integration method we use is Heun's method with a discrete-time step $\mathrm{d}t = 0.01$. For each realization, we disregard the first 2×10^5 steps to avoid any transient behavior. The step interval of sample microstates in the ensemble matrix is 50 and their recorded step number is 20000 in total, i.e., $M = 20000$.

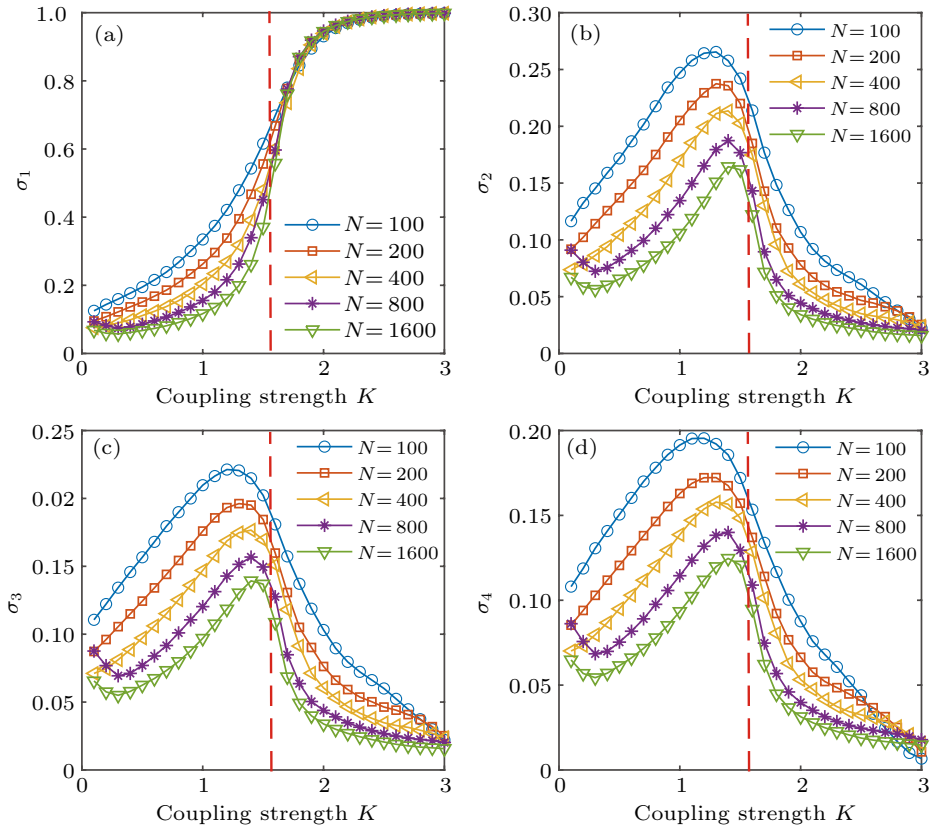


Fig. 2. (a)–(d) The first to fourth eigenvalues of the Kuramoto model against the coupling strength K.

As presented in Fig. 2(a), there is a condensation of the first eigen microstate and a phase transition with the increase of coupling strength. The second to fourth eigenvalues near the phase transition point are shown in Figs. 2(b)–2(d). The spatial distributions and temporal behaviors of eigen microstates will be discussed in Section 4. Using the fixed-point property of the eigenvalue ratio, we verify the consistency of the critical point obtained from the EMT with the MFA by the top ten eigenvalues shown in Fig. 2.

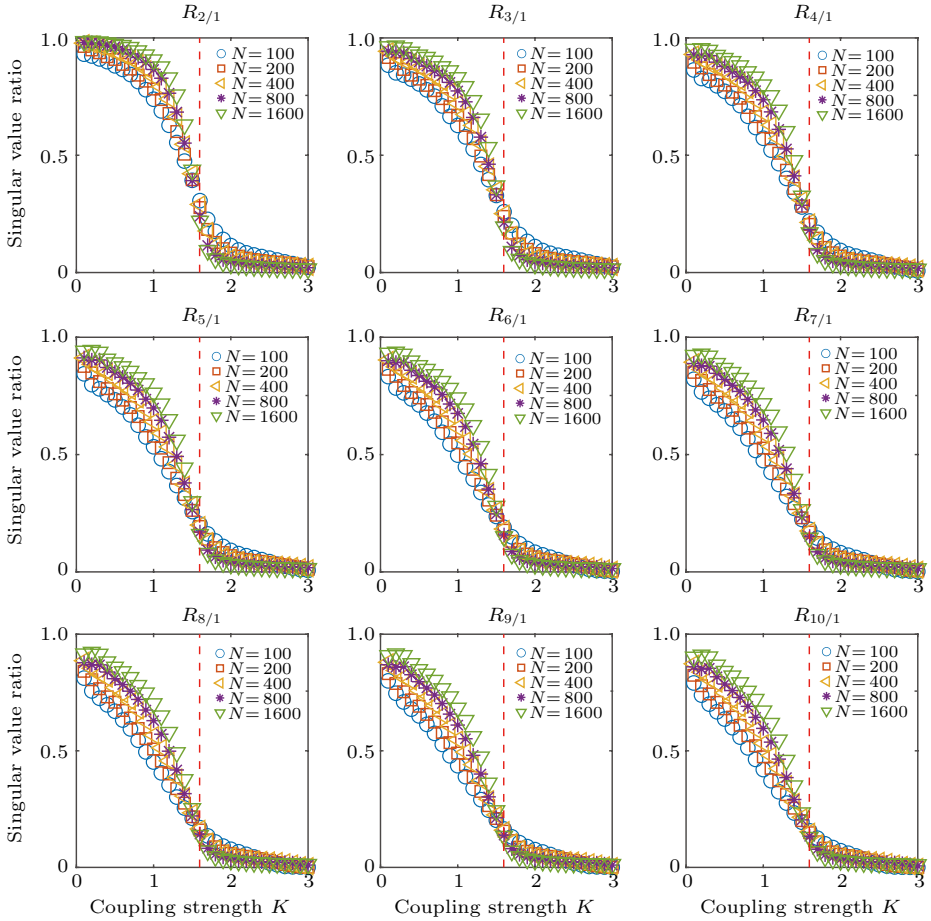


Fig. 3. Eigenvalue ratio σ_I/σ_1 versus the coupling strength K for different system sizes from $N = 100$ to $N = 1600$. The vertical dashed red line represents the fixed point corresponding to K_c.

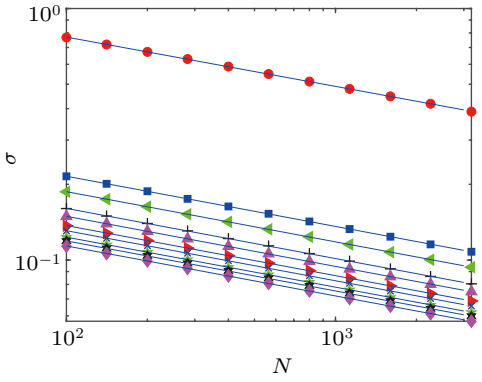


Fig. 4. The log–log plot of eigenvalues from σ_1 to σ_{10} at $K_c = \sqrt{8/\pi}$ versus system size N. The weight of these eigen microstates is $\sum_{i=1}^{10}\sigma_i^2 > 90\%$.

Table 1. Values of $\beta/\bar{\nu}$ obtained from Eq. (16) and β calculated with $\bar{\nu} = 5/2$.

σ	$\beta/\bar{\nu}$ (standard error)	β (standard error)
σ_1	0.2088 ($\pm$ 0.0334)	0.5220 ($\pm$ 0.0835)
σ_2	0.1952 ($\pm$ 0.0381)	0.4880 ($\pm$ 0.0953)
σ_3	0.1958 ($\pm$ 0.0288)	0.4895 ($\pm$ 0.0720)
σ_4	0.1955 ($\pm$ 0.0344)	0.4888 ($\pm$ 0.0860)
σ_5	0.1983 ($\pm$ 0.0309)	0.4958 ($\pm$ 0.0773)
σ_6	0.2076 ($\pm$ 0.0302)	0.5190 ($\pm$ 0.0755)
σ_7	0.2053 ($\pm$ 0.0298)	0.5132 ($\pm$ 0.0745)
σ_8	0.1982 ($\pm$ 0.0295)	0.4955 ($\pm$ 0.0738)
σ_9	0.2034 ($\pm$ 0.0265)	0.5085 ($\pm$ 0.0663)
σ_{10}	0.1957 ($\pm$ 0.0285)	0.4893 ($\pm$ 0.0713)

At the phase transition point, the FSS form $\sigma_I = N^{-\beta/\bar{\nu}} f_I(0)$ can be used to determine the critical exponent ratio $\beta/\bar{\nu}$ from the slope of its log–log plot, as presented in Fig. 4. Further, the FSS of $R_{I/1}$ can be realized with $\bar{\nu} = 5/2$ in Fig. 5. These critical exponent values agree with the previous results[32–37] with

$$\beta = \tfrac{1}{2}, \quad \beta/\bar{\nu} = \tfrac{1}{5}, \quad \bar{\nu} = \tfrac{5}{2}, \tag{19}$$

which precisely ensures that the top nine eigenvalues meet the scale invariance shown in Fig. 6.

In addition, we investigate the average modulus $\langle\Delta\rangle$, which is supposed to satisfy the FSS form[34,38]

$$\langle\Delta\rangle(K,N) = N^{-\beta/\bar{\nu}} f(\varepsilon N^{1/\bar{\nu}}). \tag{20}$$

The results of $\langle\Delta\rangle$ and its FSS form are presented in Fig. 7. We can see that $\langle\Delta\rangle$ is obviously different from σ_1 of the first eigen microstate, even though they both satisfy the FSS. Since the Kuramoto model is not in equilibrium, the emergent phase of the system can evolve over time. Time-averaged quantities cannot precisely characterize the order parameter. According to the EMT, the emergence of phase can be identified by the condensation of eigen microstate U_I with finite eigenvalue σ_I, which serves as its order parameter. The dynamics of phase U_I is described by V_I.

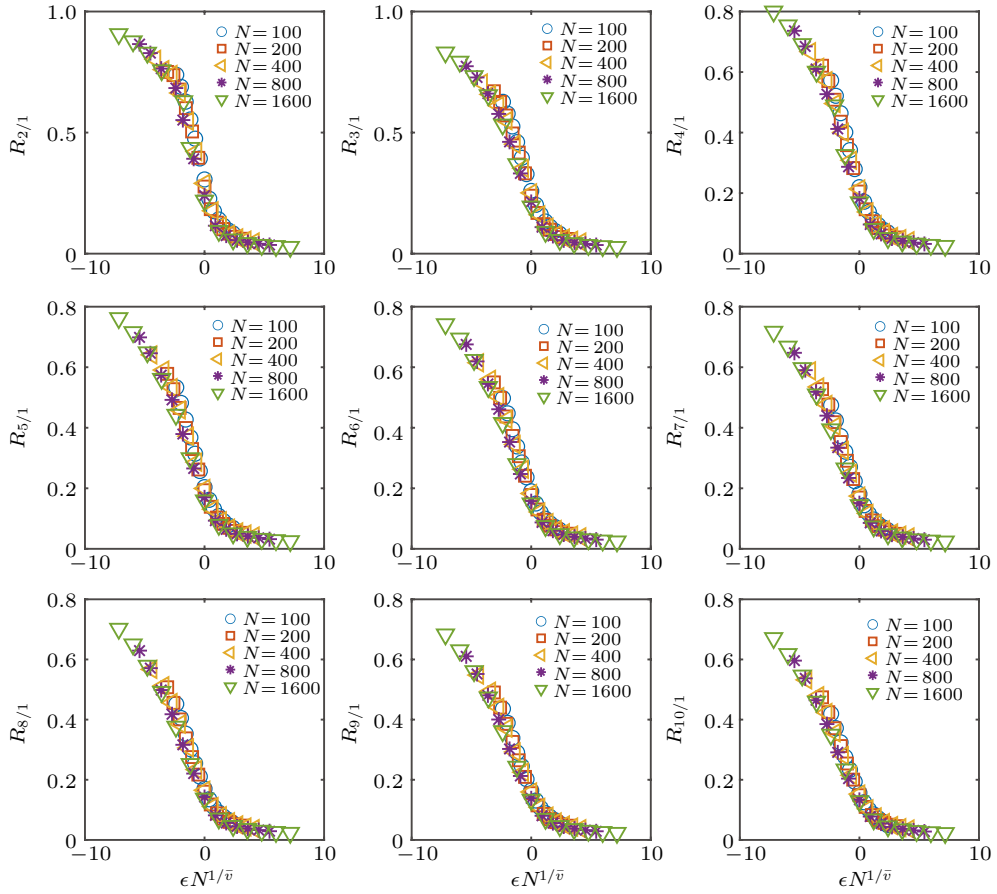


Fig. 5. The finite-size scaling of eigenvalue ratios σ_I/σ_1 for $I = 2, 3, \ldots, 10$ in the range $\varepsilon = [-0.375, 0.375]$.

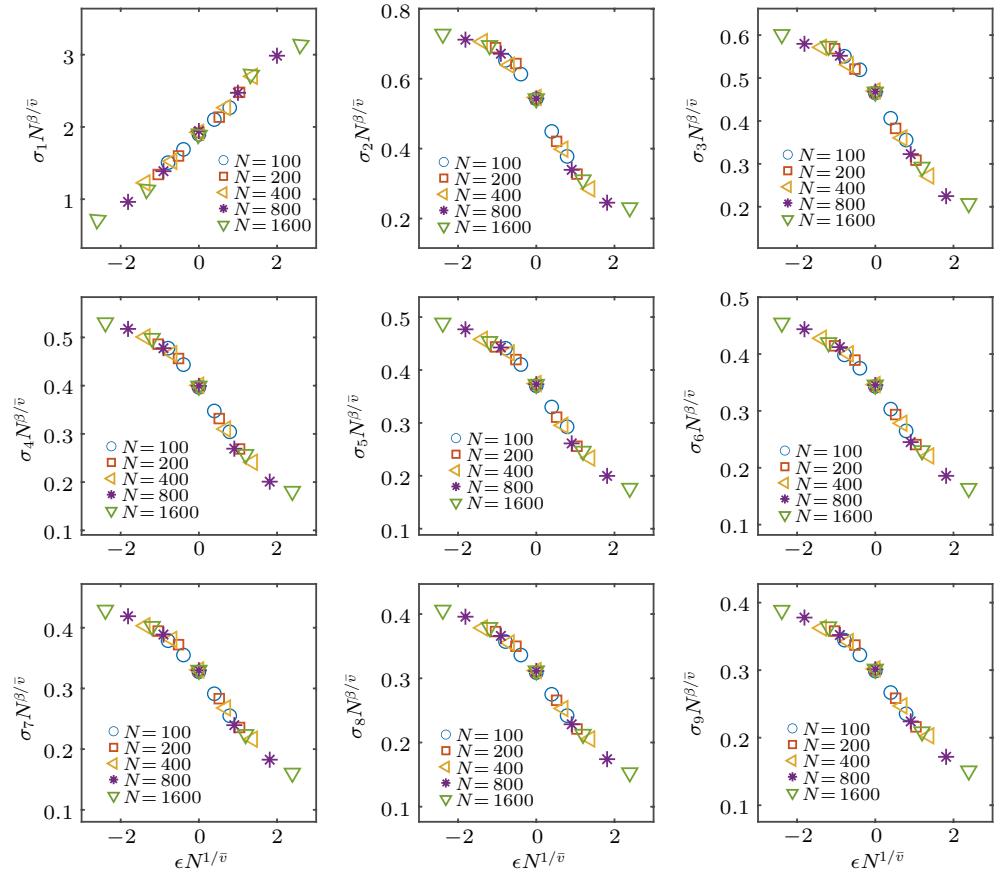


Fig. 6. The finite-size scaling of eigenvalues σ_1–σ_9 in the range $\varepsilon = [-0.125, 0.125]$.

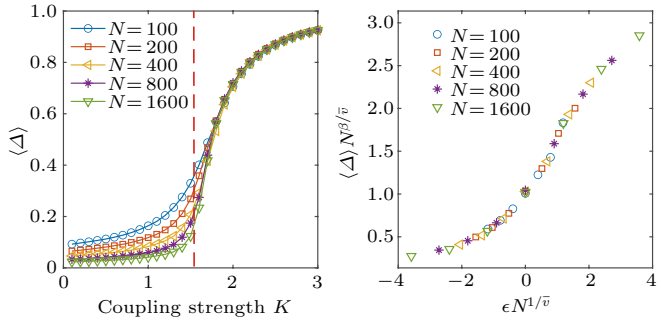


Fig. 7. (a) The average Kuramoto modulus $\langle\Delta\rangle$ against coupling strength K. (b) The finite-size scaling form of $\langle\Delta\rangle$ in the range $\varepsilon=[-0.125,0.125]$.

4. Spatial distributions and temporal behaviors of eigen microstates

4.1. Spatial distributions of eigen microstates

The spatial distribution of the I-th eigen microstate is characterized by $\boldsymbol{U}_I=\left(u_1^I,u_2^I,\ldots,u_N^I\right)^{\mathrm{T}}$, where $u_i^I=\Delta_i^I\left(\cos\theta_i^I,\sin\theta_i^I\right)$. In Fig. 8(a), we show the phase θ_i^I of oscillator i versus its intrinsic frequency ω_i for $I=1,2,3$. The results of negative to positive intrinsic frequencies are presented using blue, green, yellow to red colors successively. At the subcritical state with $K=0.1$, the phases of all oscillators with different frequencies are randomly distributed. At the critical state with $K=K_{\mathrm{c}}$, the phases of the first eigen microstate $\boldsymbol{U}_1$ become partially synchronized. The phases of the top three eigen microstates are partially synchronized in the supercritical state with $K=3$.

The amplitudes Δ_i^I of oscillator i are presented in Fig. 8(b) for $I=1,2,3$. At the subcritical state $K=0.1$, there is a bimodal distribution of amplitude around $\omega=\pm\pi/2$. At the critical state $K=K_{\mathrm{c}}$, the distribution of amplitude for U_1 is centralized around $\omega=0$ and the second and third eigen microstates still have a bimodal distribution of amplitude. In the supercritical state, the amplitudes of oscillators with frequencies between $\omega\approx-\pi$ and $\omega\approx\pi$ are almost the same in the first eigen microstate of synchronization. For the second and third eigen microstates, only the amplitudes of oscillators with $|\omega|\approxeq\pi$ are obviously nonzero.

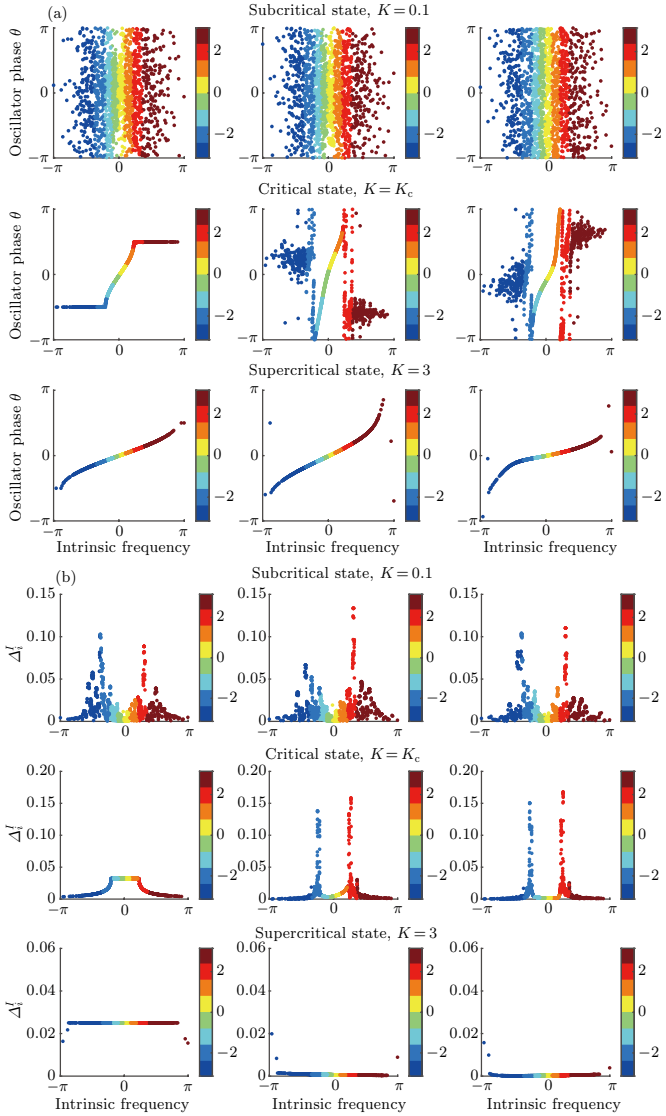


Fig. 8. Phases and amplitudes of all oscillators with different frequencies for the top three eigen microstates.

4.2. Temporal behaviors of eigen microstates

The temporal evolution of eigen microstate $\boldsymbol{U}_I$ is characterized by its eigen dynamic microstate $\boldsymbol{V}_I$. In Fig. 9, we show the top three eigen dynamic microstates versus time at subcritical, critical and supercritical states. Their Fourier spectra are presented in Fig. 10. With the condensation of the first

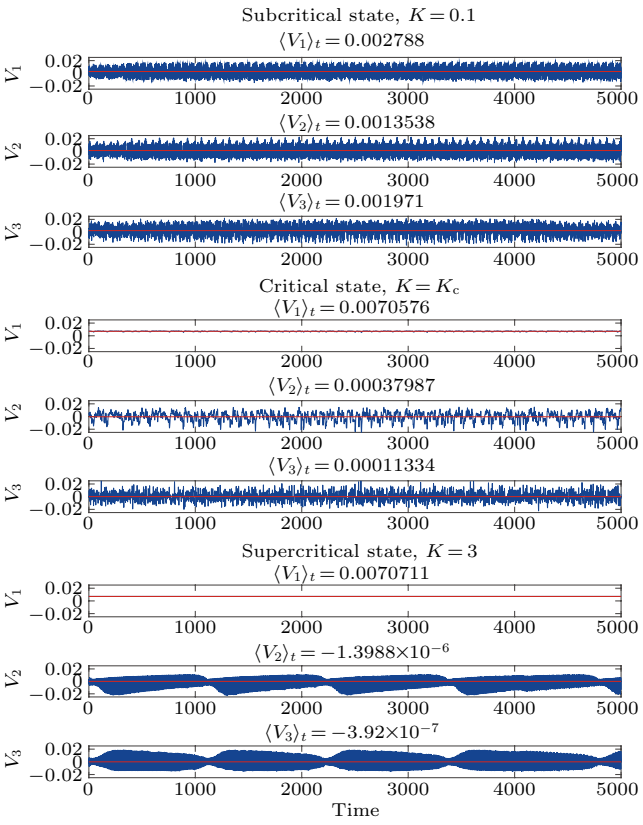


Fig. 9. The temporal evolution of the top three eigen dynamic microstates at subcritical, critical and supercritical states. Here the red line represents the average of the time evolution of each eigen microstate.

eigen microstate $\boldsymbol{U}_1$ at $K = K_c$, there is also a condensation of the Fourier spectrum at zero frequency for the first eigen dynamic microstate $\boldsymbol{V}_1$. An interesting phenomenon is observed for $K = 3$ that the drifting oscillators do not move randomly, as shown in the second and third eigen microstate in Fig. 9. The spectral analysis reveals that these oscillators exhibit a long periodic motion and maintain high-frequency motion within each period.

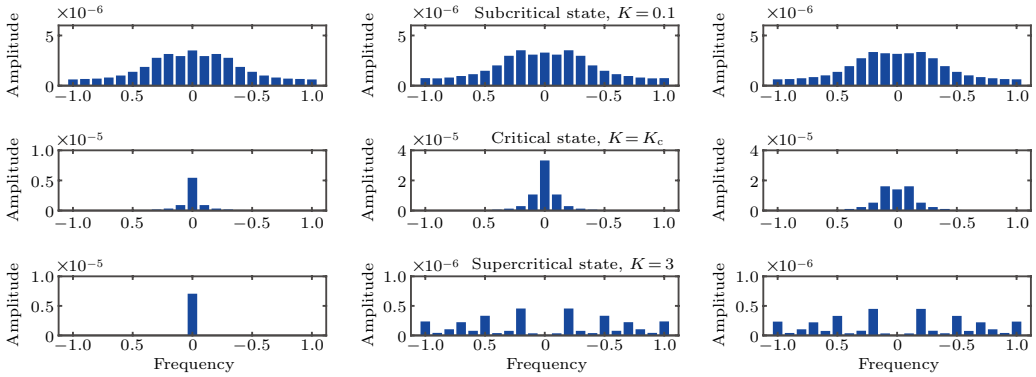


Fig. 10. The Fourier spectrums of the top three eigen dynamic microstates at subcritical, critical and supercritical states.

5. Conclusion

In this paper, we apply the EMT to study the critical behaviors of the Kuramoto model, which is a classical model of synchronization. Beyond the MFA, which measures the oscillator synchronization by the offset of the oscillator phase barycenter, we further investigate the phase fluctuations from the barycenter of oscillators using the EMT. We define a microstate of the Kuramoto model with the phase fluctuations of all oscillators. From all microstates during the time interval under investigation, we can construct a statistical ensemble. Then, we can calculate the eigen microstates, their temporal evolutions, and the corresponding eigenvalues, the squares of which represent their weights in the ensemble. Before the emergence of synchronization, all eigenvalues are very small and there is no dominant eigen microstate. With an increase in coupling strength, the largest eigenvalue σ_1 becomes finite. Then there is a condensation of eigen microstate and emergence of the phase $\boldsymbol{U}_1$ with the order parameter σ_1, which satisfies the finite-size scaling law in the critical regime.

We have also studied the temporal behaviors of eigen microstates. Before synchronization, the temporal evolution $\boldsymbol{V}_1$ of the largest eigen microstate $\boldsymbol{U}_1$ exhibits a wide range of frequencies. After the synchronization, with the condensation of $\boldsymbol{U}_1$, there is also a condensation at zero frequency in its temporal evolution $\boldsymbol{V}_1$.

In conclusion, we have successfully applied the eigen microstate theory to study the mesoscopic to global critical behaviors of the Kuramoto model beyond the MFA. Using this theory, we can study the synchronization and its precise critical behaviors for general oscillator systems, which have critical exponents different from that of MFA.

Acknowledgements

The authors would like to thank Dr Teng Liu, Dr Xiaojie Chen, Dr Gaoke Hu and Dr Jiaqi Dong for the insightful and valuable discussions. This work is supported by the National Natural Science Foundation of China (Grant Nos. 12135003, 71731002, and 12471141), the Postdoctoral Fellowship Program of CPSF (Grant No. GZC20231179), the China Postdoctoral Science Foundation–Tianjin Joint Support Program (Grant No. 2023T001TJ), and the Tianjin Education Commission scientific Research Project (Grant No. 2023SK070).

References

[1] Ikeda Y, Aoyama H, Fujiwara Y, Iyetomi H, Ogimoto K, Souma W and Yoshikawa H 2012 *Progress of Theoretical Physics Supplement* **194** 111
[2] Wilson C J and Callaway J C 2000 *Journal of Neurophysiology* **83** 3084
[3] Martens E A, Thutupalli S, Fourriere A and Hallatschek O 2013 *Proc. Natl. Acad. Sci. USA* **110** 10563
[4] Doelling K B, Assaneo M F, Bevilacqua D, Pesaran B and Poeppel D 2019 *Proc. Natl. Acad. Sci. USA* **116** 201816414
[5] Kralemann B, Fruhwirth M, Pikovsky A, Rosenblum M, Kenner T, Schaefer J and Moser M 2013 *Nat. Commun.* **4** 2418
[6] Ott E and Antonsen T M 2008 *Chaos* **18** 037113
[7] Strogatz S H 2000 *Physica D* **143** 1
[8] Acebron J A, Bonilla L L, Vicente C P, Ritort F and Spigler R 2005 *Rev. Mod. Phys.* **77** 137
[9] Oh E, Lee D, Kahng B and Kim D 2007 *Phys. Rev. E* **75** 011104
[10] Sakaguchi H 2000 *Phys. Rev. E* **61** 7212
[11] Miritello G, Pluchino A and Rapisarda A 2009 *Europhys. Lett.* **85** 10007
[12] Moloney D and Nicholas R 2005 *Complexity and Criticality* (Imperial College Press)
[13] Li X T and Chen X S 2016 *Commun. Theor. Phys.* **66** 355
[14] Zhang X, Hu G, Zhang Y, Li X and Chen X 2018 *Science China-physics Mechanics and Astronomy* **61** 120511
[15] Hu G K, Liu T, Liu M X, Chen W and Chen X S 2019 *Science China Physics, Mechanics and Astronomy*
[16] Sun Y, Hu G, Zhang Y, Lu B, Lu Z, Fan J, Li X, Deng Q and Chen X 2021 *Commun. Theor. Phys.* **73** 065603
[17] Li X, Xue T T, Sun Y, Fan J F, Li H, Liu M X, Han Z G, Di Z R and Chen X S 2021 *Chin. Phys. B* **30** 128703

[18] Liu T, Hu G K, Dong J Q, Fan J F, Liu M X and Chen X S 2022 *Chin. Phys. Lett.* **39** 080503

[19] Zhang Y, Liu M, Hu G, Liu T and Chen X 2024 *Phys. Rev. E* **109** 044130

[20] Hu G, Sun Y, Liu T, Zhang Y, Liu M, Fan J, Chen W and Chen X 2023 *Science China Physics, Mechanics & Astronomy* **66** 120511

[21] Chen X, Ying N, Chen D, Zhang Y, Lu B, Fan J and Chen X 2021 *Chaos* **31** 071102

[22] Sun Y, Meng J, Yao Q, Saberi A A, Chen X, Fan J and Kurths J 2021 *Phys. Rev. E* **104** 064139

[23] Wang N N, Qiu S H, Zhong X W and Di Z R 2023 *Applied Mathematics and Computation* **449** 127924

[24] Wang N N, Wang Y J and Di Z R 2024 *Chaos, Solitons & Fractals* **188** 115519

[25] Huo S and Liu Z 2023 *Communications Physics* **6** 285

[26] Chen X, Ren H, Tang Z, Zhou K, Zhou L, Zuo Z, Cui X, Chen X, Liu Z, He Y, *et al*. 2023 *Communications Biology* **6** 892

[27] Zheng Z, Xu C, Fan J, Liu M and Chen X 2024 *Chaos* **34** 022101

[28] Moyal B, Rajwani P, Dutta S and Jalan S 2024 *Phys. Rev. E* **109** 034211

[29] Li X, Zhang J, Zou Y and Guan S 2019 *Chaos* **29** 043102

[30] Skardal P S, Ott E and Restrepo J G 2011 *Phys. Rev. E* **84** 036208

[31] Lepri S and Ruffo S 2001 *Europhys. Lett.* **55** 512

[32] Hong H, Park H and Choi M 2005 *Phys. Rev. E* **72** 036217

[33] Hong H, Chaté H, Park H and Tang L H 2007 *Phys. Rev. Lett.* **99** 184101

[34] Hong H, Chate H, Tang L and Park H 2015 *Phys. Rev. E* **92** 022122

[35] Daido H 2015 *Phys. Rev. E* **91** 012925

[36] Tang L H 2011 *J. Stat. Mech.: Theory and Experiment* **2011** P01034

[37] Hong H, Um J and Park H 2013 *Phys. Rev. E* **87** 042105

[38] Um J, Hong H and Park H 2014 *Phys. Rev. E* **89** 012810